Korean J. Chem. Eng., **27**(5), 1404-1411 (2010)
DOI: 10.1007/s11814-010-0232-5

Combined experimental and kinetic modeling studies for the conversion of gasoline range hydrocarbons from methanol over modified HZSM-5 catalyst

Hasan Akhtar Zaidi*,† and Kamal Kishore Pant**

*University School of Chemical Technology, Guru Gobind Singh, Indraprastha University, Kashmere Gate, Delhi-110006, India
**Department of Chemical Engineering, Indian Institute of Technology Hauz Khas, Delhi-110016, India
(*Received 10 September 2009 • accepted 8 December 2009*)

Abstract−The reaction was carried out in fixed bed reactor. The effect of process variables on the activity of oxalic acid treated 0.5 wt% ZnO/7 wt% CuO/HZSM5 catalyst for the conversion of methanol to gasoline range hydrocarbons was studied. The catalyst was prepared by incipient wetness impregnation method. After impregnation the catalyst was treated with oxalic acid. The validity of kinetic model proposed for the methanol to gasoline range hydrocarbon process at zero time on stream was studied, from the experimental results obtained in a wide range of operating conditions. The kinetic parameters for various models were calculated by solving the equation of mass conservation in the reactor for the lumps of the kinetic models. The kinetic model fitted well for simulating the operation in the fixed bed reactor in the range of 635 to 673 K,with regression coefficient (R^2) higher than 0.96.

Key words: HZSM-5, ASTM Distillation Curve, Methanol to Gasoline, Initial Boiling Point, Final Boiling Point

INTRODUCTION

The conversion of methanol to gasoline range hydrocarbons has attracted many researchers due to the increase in crude oil prices. Methanol feed in the MTG process can be derived from coal or natural gas based syngas. The MTG process involves the conversion steps of syngas-to-methanol and methanol-to-gasoline. The high surface area associated with the zeolites allows a high degree of dispersion of active metals over the zeolites, making maximum use of the metal deposited. The pentasil ZSM-5 was investigated as catalyst for methanol conversion to hydrocarbons [1-8]. The effect of temperature, space velocity and pressure on the methanol conversion and hydrocarbons yields was studied [3]. The effect of partial pressure of methanol on the relative rates of dehydration and aromatization steps in the reaction [4] was considered. The effect of space-time on the methanol conversion and hydrocarbon products distribution indicates that C_2-C_4 olefins are the intermediates in MTG reactions [4,9]. Researchers have reviewed the proposed reaction mechanism for the methanol to hydrocarbons and identified the activity and selectivity relationships [9-11]. It has been reported that in the conversion of methanol to hydrocarbons, up to 70% selectivity to C_2-C_4 olefins at 100% conversion over ZSM-5 class zeolites can be achieved [12]. The yield of light olefins increases with space-time and reaches maximum, indicating the intermediate character of the light olefins formed. An important feature of the methanol to hydrocarbons reaction on ZSM-5 is that increase of space-time results in a continuing change of hydrocarbon distribution [13-16].

[17] reviewed the process technology for the conversion of methanol to hydrocarbons. Methanol conversion and hydrocarbon yield increases using HZSM-5 with the attainment of an optimal temperature of 673 K. Ga_2O_3 impregnated HZSM-5 catalyst remarkably increases the selectivity to aromatics at the expense of C_2-C_4 alkenes without affecting the overall conversion [18]. At higher temperature, olefin formation was favored with respect to the formation of aromatics. Thermodynamically, the effect of increasing the temperature over the same range of partial pressures of olefins is to shift the distribution towards lower hydrocarbons. At methanol pressure below 20 kPa, the selectivity of aromatics decreased with the increasing methanol pressure. The partial pressure of methanol has been a strong influence on the olefin selectivity. The decrease in partial pressure tends to enhance the olefin formation and suppress the aromatization reaction of olefins [19].

Several investigators have reported the influence of the synthesis condition of HZSM-5 on the selectivity towards light olefins and aromatics [15,18]. Lowering the aluminum content at the outer shell improves the catalyst properties and provide sites, which are highly selective to gasoline range [20].

Kinetic investigations related to the methanol to hydrocarbons conversion normally consider the methanol-dimethyl ether mixture as a single species. This seems to be justified, since the dimethyl ether formation is much faster than the subsequent reactions, so that oxygenates are at equilibrium [4,9,21-23]. Based on the autocatalytic nature of the methanol conversion over ZSM-5, a proposed a kinetic model, which takes into account the rate of disappearance of oxygenates, accelerated by their reaction with olefins [24]. Fitting experimental data obtained on H-ZSM-5 with varying concentrations of acid sites showed a linear correlation between the rate constant of the reaction of oxygenates with olefins and the intrinsic acid activity of the catalyst [25].

The model shows olefins as a primary product and proposed reactions between oxygenates and olefins as autocatalytic steps [24]. This model was modified by adding a bimolecular step accounting for the carbene insertion in the primary olefins [9].

According to the model, dimethyl ether and methanol are at equilibrium at all times in the reactor [26]. Once the dimethyl is formed,

†To whom correspondence should be addressed.
E-mail: hasan.azaidi@gmail.com

it can react to form light olefins (ethylene and propylene), which can polymerize to form products of gasoline range. These products can react with DME/MeOH or form more light olefins to produce additional gasoline products. A kinetic model was proposed for the methanol to olefins (MTO) process on the catalyst based on silicoaluminophosphate SAPO-34 [27]. A detailed study was done on a kinetic model for methanol conversion to hydrocarbons over zeolites [28]. The overall reaction scheme contained 53 reactions based on radical reactions.

In the present research, the oxalic acid treated ZnO/CuO/HZSM-5 catalyst has been prepared for the production of gasoline range hydrocarbons from methanol. Previous investigation [29-31] revealed the effect of CuO and ZnO loading on HZSM-5 catalyst for the conversion of methanol to hydrocarbons. The results indicate 0.5 wt% ZnO/7 wt%CuO/HZSM-5 had higher conversion and hydrocarbon yields as compared to other catalyst. Experimental runs were conducted to study the effect of process variables such as temperature, contact time and partial pressure on methanol conversion and hydrocarbons yield. The kinetic data were obtained from the experimental runs. The kinetic parameters for the various models were calculated by solving the equation of mass conservation in the reactor for the lumps of kinetic models. The validity of the models proposed in the literature was analyzed.

EXPERIMENTAL

0.5wt%ZnO/7wt%CuOHZSM-5 catalyst was prepared by wet impregnation method. The details of this catalyst preparation are given elsewhere [29]. [HZ (Zn/Cu)] catalysts with 1 molar oxalic acid were dissolved in deionized water for 2 minutes at 353 K. The treated particles were washed thoroughly with deionized water and finally dried over night at 393 K in an oven.

The surface areas and pore volumes of the catalysts were determined by using ASAP 2010 (Micromeritics, USA) by adsorption with nitrogen (99.99% purity) at 77 K, employing the static volumetric technique. Prior to the analysis the catalysts samples were degassed for 6 h at 383 K under vacuum. With the gradual increase in pressure, the number of gas molecules adsorbed on the surface increased. Analysis of the adsorption isotherm was done with the help of a software (ASAP 2010) and the information about the distribution of pore size and surface area of the catalyst was obtained.

To determine the actual amount of CuO and ZnO doped over HZSM-5, and the Si/Al ratio, the catalyst samples were digested with nitric acid at 353 K for 2 h under reflux. The final metal content of the catalyst was determined with a metal trace analyzer (Metrohm 757 VA Computrace, Switzerland).

With ASTM test procedures, the properties of Indian gasoline and gasoline obtained by MTG (Methanol to gasoline) process were tested by Reid vapor pressure and ASTM distillation. Key distillation properties for gasoline were derived from ASTM D-86. Reid vapor pressure (RVP) of a fuel is defined by ASTM test procedure D 5191. These various test methods ultimately obtained an estimate of partial pressure of gasoline component at 100 °F in a vessel with a 4/1 vapor to liquid volume ratio.

For experiments the catalyst pellets were crushed and sieved to obtain a particle size in the range of 2.5±0.5 mm. The details of experimental setup and procedure have been discussed in the previous paper [29]. The tubular reactor was made of a stainless steel tube (id: 0.019 m). The reactor was heated in three zones by means of electric furnace, and temperature was varied from 635 K-698 K during the run. To minimize the heat losses between the preheater and reactor, the bare length of the tube was properly insulated with magnesia wool. The contact time was varied between 0.047 to 0.129 (g of catalyst) h (g of methanol fed)$^{-1}$. During experimental runs, the total condensed liquid and gases were analyzed to determine the composition of non-condensable gases and liquid at regular intervals. The non-condensable gases contained mainly C_1 to C_5 hydrocarbons; CO and CO_2 were trapped in sampling valves and analyzed by gas chromatography. All the liquid hydrocarbon products were analyzed by flame ionization detector using a chromatograph (Aimil-Nucon, India).

RESULTS AND DISCUSSION

The physicochemical properties of liquid product analyzed as per ASTM methods were specific gravity, Reid vapor pressure and ASTM distillation curve. The amounts of light and heavy components present in the gasoline were monitored by the use of ASTM distillation curve following norm D86 as shown in Fig. 1. The most important points of the distillation curve are initial boiling point (IBP), T_{10} (temperature at which 10% of distilled volume is recovered), T_{50} (temperature at which 50% of distilled volume is recovered), T_{90} (temperature at which 90% of distilled volume is recovered) and final boiling point (FBP). A typical ASTM results and other properties for liquid products obtained were compared with properties of Indian gasoline. The results are given in Table 1. The properties of liquid products obtained were comparable with the gasoline.

The crystallite size, which results in more sites of CuO available

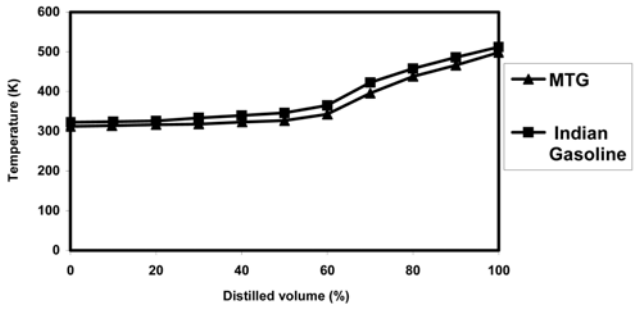

Fig. 1. Typical ASTM distillation curve for indian gasoline and MTG process gasoline.

Table 1. Physicochemical properties of the product

Sample	Specific gravity at 293 K	Reid vapor pressure (kPa)	IBP (K)	T_{10} (K)	T_{50} (K)	T_{90} (K)	FBP (K)
Indian gasoline	0.7608	42.9	322.7	324.0	346.0	486	512.4
MTG product	0.752	44.5	312	314.0	335.2	466.0	498.2

for methanol adsorption thereby, increases the activity of the catalyst [29]. Mild treatment of CuO/ZnO impregnated HZSM-5 catalyst with oxalic acid has beneficial effect on the reaction, owing, on the one hand, to the removal of extra framework aluminum species which act as poison of the Bronsted acidic sites, and the other hand, to increase of external surface area of catalyst which allows easier access of the reactant to the active sites and leads to more resistance to deactivation [20]. Based on above investigations it was concluded that oxalic acid treated 0.5 wt%ZnO/6.89 wt%CuO/HZSM-5 catalyst abbreviated as HZ (Ox) has higher activity and selectivity for methanol transformation to gasoline range hydrocarbons. The conversion capacity was estimated at various reactant feed rates and temperatures. 673 K was the optimum temperature to obtain the higher yield of gasoline range hydrocarbons. Therefore, this catalyst was used for detailed kinetic studies. These results are discussed below:

Experimental runs were conducted at different contact time (W/F_{A0}) and temperatures. Figs. 2 and 3 show the effect of contact time and temperatures for methanol conversion and hydrocarbons yield, respectively. Both methanol conversion and total hydrocarbons yield increases progressively on increasing W/F_{A0} from 0 to 0.129 (g. cat*h/g methanol fed). Figs. 4 and 5 show the variation in product distribution as a function of contact time at three different temperatures, 635 K, 653 K, 673 K, respectively. The yield of aromatic hydrocarbons increased with increase in the contact time or conversion while the yield of lighter olefins decreased. At low conversion a high yield of olefins and DME was obtained and negligible yield of aromatics was formed. Fig. 6 shows the major hydrocarbon product distribution such as olefins, alkanes, aromatics and C_{5+} on water-free basis at various contact time. A detailed product distribution is also given in Table 2 at different temperatures and contact time. The results show that olefins and DME are the intermediates to aromatics and in agreement with the published literature [28-32].

The yield of aromatics increased with increase in contact time, while the yield of olefins and DME gradually decreased with increase in contact time, indicating that alkenes (olefins) and DME are the

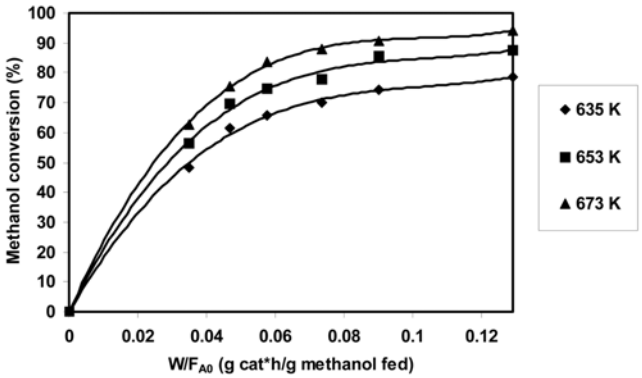

Fig. 2. Variation of methanol conversion with contact time over HZ (Ox) catalyst.

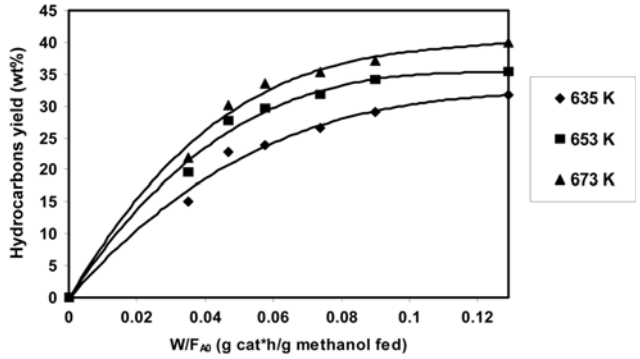

Fig. 3. Variation of hydrocarbons yield with contact time over HZ (Ox) catalyst.

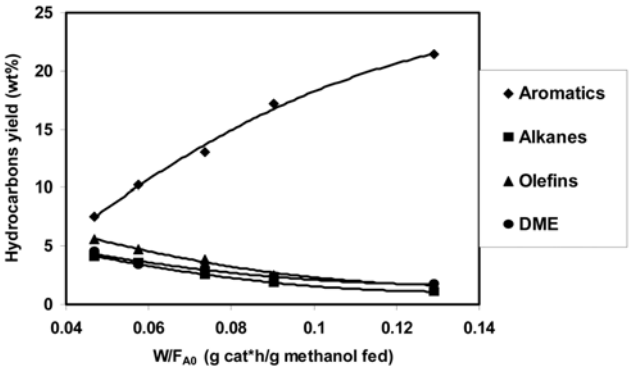

Fig. 4. Hydrocarbons yield vs contact time over HZ (Ox) catalyst [T=635 K, P=1 atm].

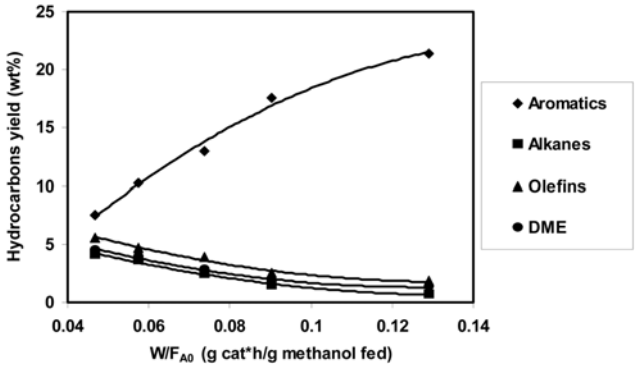

Fig. 5. Hydrocarbons yield vs contact time over HZ (Ox) catalyst [T=653 K, P=1 atm].

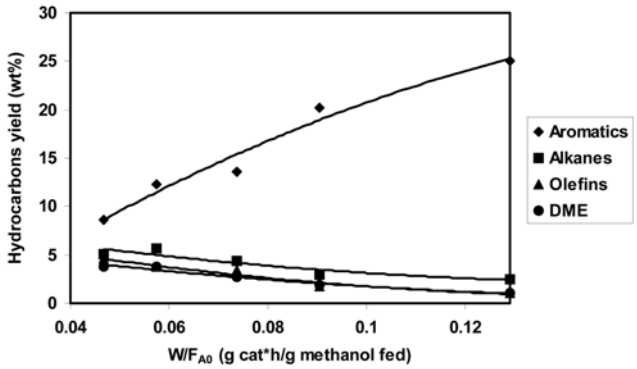

Fig. 6. Hydrocarbons yield vs contact time over HZ (Ox) catalyst [T=673 K, P=1 atm].

Table 2. Products distribution for the conversion of methanol to gasoline range hydrocarbons over HZ (Ox) catalyst (P=1 atm)

	T=635 K			T=653 K			T=673 K			T=698 K		
W/F_{A0} (g cat.*h/g of methanol fed)	0.129	0.090	0.047	0.129	0.090	0.047	0.129	0.090	0.047	0.129	0.090	0.047
Conversion (%)	80.7	74.3	61.6	87.5	82.5	69.5	94.2	90.8	75.4	83.9	75.2	58.7
Yield (wt%)												
CH_4	0.34	0.37	1.03	0.25	0.36	0.92	0.15	0.31	0.82	0.40	0.45	0.98
C_2	1.0	0.92	2.10	0.72	1.04	2.38	0.52	0.89	1.82	3.20	2.32	1.20
C_3	1.17	1.25	3.98	0.84	1.22	3.56	0.69	1.05	3.23	4.31	3.41	2.80
C_4	0.55	0.77	2.46	0.41	0.60	2.26	0.60	0.51	2.15	0.82	0.92	0.09
C_5	0.40	0.78	1.40	0.54	0.63	1.37	0.68	0.58	0.90	0.32	0.38	1.30
C_5+	12.29	11.03	3.50	11.80	10.60	4.90	11.50	10.57	8.20	13.20	11.83	6.80
C_6H_6	0.33	0.29	0.38	1.23	1.11	0.06	0.33	0.44	0.68	0.18	0.13	0.07
C_7H_8	0.36	0.24	0.12	0.26	0.24	0.02	2.87	1.75	0.08	0.20	0.16	0.09
C_8H_{10}	6.73	5.08	1.40	8.86	8.21	2.72	10.47	9.30	4.32	4.73	2.82	1.12
C_9H_{12}	6.11	5.54	1.20	7.79	7.0	3.94	10.76	9.40	5.45	2.11	1.42	0.07
$C_{10}H_{14}$	0.38	0.31	0.02	1.09	0.80	0.10	0.44	0.35	0.41	0.21	0.16	0.05
CH_3OCH_3	2.11	2.43	5.15	1.55	2.25	5.40	1.04	1.94	3.77	3.11	3.42	4.50
Total hydrocarbons products (wt% feed)	31.77	29.01	22.74	35.34	34.06	27.63	40.05	37.09	31.83	32.79	27.42	19.07
Water (wt% feed)	30.0	28.0	21.80	34.20	32.15	24.44	37.2	35.15	24.44	30.20	25.32	20.20
*Others (wt% feed)	18.91	17.28	17.08	17.92	16.31	17.42	16.98	18.54	19.17	20.95	22.43	19.40

*Include CO and CO_2

intermediates to aromatics [9,10,17]. Yield of alkanes also decreased at higher conversion. As can be seen from Table 2, significant amounts of liquid hydrocarbons were obtained with HZ (Ox) catalyst. At higher temperatures up to 673 K the methanol conversion and liquid products increased. The major gaseous products of the reaction were methane, ethylene, dimethyl ether, propylene, butane and pentane. The major liquid products were pentane, ethyl benzene, ethyl toluene, trimethyl benzene and tetramethyl benzene, at all temperatures and conversion levels.

Experimental runs were conducted at different temperature to study the effect of temperature on methanol conversion and yield of hydrocarbons over CuO impregnated HZSM-5 catalyst treated with oxalic acid. Experimental data revealed several interesting qualitative MTG reactions. As shown in Fig. 7 there was increase in the yield of C_{5+} and mainly aromatic hydrocarbons with increase in temperature from 635 K to 673 K. It was observed, based on the

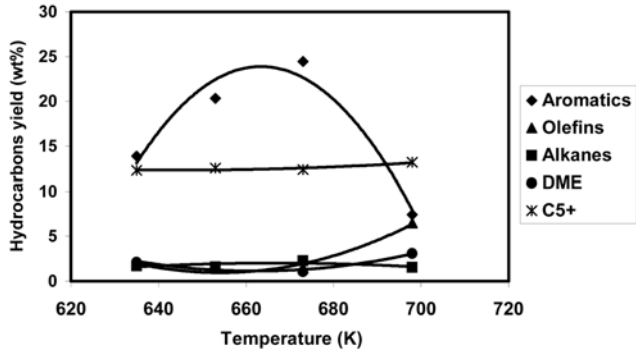

Fig. 7. Effect of reaction temperature on hydrocarbons yield [W/F_{A0} (g cat*h/g of methanol fed)=0.129, P=1 atm].

experimental results, that 635 K to 673 K is the most appropriate temperature range for the selective transformation of methanol to aromatic hydrocarbons. As the reaction temperature increased, oligomerization, cyclization, dehydrogenation and aromatization reactions progress and olefins were converted into the higher hydrocarbons. The distribution of aromatics also changed strongly with increasing temperature. The methanol reaction is comprised of secondary reaction that converts primary olefins product to gasoline range hydrocarbons. At 698 K the catalyst deactivated faster because of rapid coke formation over the surface. This coke formation is due to cracking of oligomers into smaller molecules and coke, which deactivates the catalyst. However, at medium temperatures oligomerization and cracking are somewhat balanced and cracking is not severe enough to make too much coke; therefore catalyst activity lasts longer. A detailed product distribution is also given in Table 2 at different temperature and contact time. A similar trend has also been reported by the other researchers [17,19]. Ethylene and propylene are generally believed to be the first olefin hydrocarbons formed during methanol conversion and they can be easily oligomerized in the temperature range from 635 K to 673 K to produce desirable hydrocarbons. These results show that CuO doped catalysts serve as highly active dehydrogenation catalyst and show a high selectivity for aromatics in the conversion of methanol.

Effect of methanol partial pressure was also investigated on conversion and hydrocarbon yields. Nitrogen was used as a dilutent. Fig. 8 represents the variation in product distribution at different partial pressures of methanol at a W/F_{A0} of 0.129 (g cat*h/g of methanol fed). When the methanol pressure was below 90 kPa, the yield of aromatic hydrocarbons was comparatively high compared to the yield of olefins and DME. Yield of aromatic hydrocarbons decreased with increase in methanol partial pressure. On the other hand, the

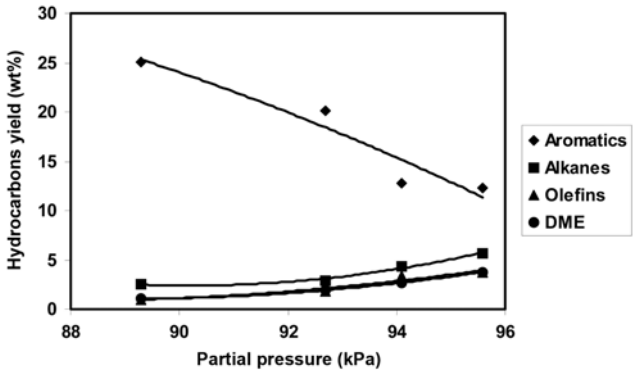

Fig. 8. Effect of methanol partial pressure on aromatics, alkane, olefins and dimethyl methyl ether yield [W/F_{A0} (g cat *h/g methanol fed)=0.129, T=673 K, P=1 atm].

yield of alkanes and olefins marginally increased with increase in methanol partial pressure. This could be due to thermodynamic limit for the dehydrogenation at high partial pressure of methanol, while at lower partial pressure of methanol dehydration and carbene ($:CH_2$) ion generation takes place. Production of aromatic hydrocarbons was favored at low methanol partial pressure, whereas the yield of alkanes, olefins and DME was favored by higher methanol partial pressure.

The kinetic models proposed in the literature can be grouped into lumped models, which are a compromise between simplicity and representations of the reality of the process, and detailed mechanistic models that take into account individual reaction steps based on radical reaction mechanism. Generally, mechanistic models involve a large number of equations and it is very difficult to estimate the rate constants for each individual reaction step. For the design purpose, molecular models (lumped parameter) are used for most of the cases [17]. In the present work the constants of kinetic models have been calculated by fitting the experimental results of mass fractions of various lumps to the corresponding mass conservation equations. The kinetic constants calculated in this way guarantees the representation of complex reaction system in the wide range of concentration of various lumps. The methodology used has been successfully applied in kinetic modeling of many catalytic reactions [25].

For the isothermal reactor and neglecting the radial concentration gradients in the reactor, the concentration terms on a water-free basis and without catalyst deactivation (activity unity) the mass conservation equation for each of the lumps at zero time on stream becomes:

$$\frac{-dc_i v}{dz} = (1-\varepsilon)\sum_{j=1}^{m} \alpha_{ij} r_{j0}; \quad i=1,m \tag{1}$$

where, α_{ij} is the stoichiometric coefficient of the i^{th} chemical species in the j^{th} reaction, c_i is the concentration of species, ε is the void fraction of the bed and v is the linear velocity. The application of the above equation requires precise calculation of the reaction rate of the formation of lump (i) at zero time on stream r_{j0}, gas linear velocity, v, and partial pressure of water-free products. To solve these ordinary differential equations, a program code was written for calculating the mass fractions of each reactant and product species. The differential equations were solved using a fourth order Runge-Kutta method. The non-linear regression technique has been carried out for the calculation of the kinetic parameters for each of the kinetic models, by minimizing the objective function.

The objective function **F(x)** to be minimized is the arithmetic mean of minimizing the square of the deviations between experimental and model predicted values of compositions of each lump.

$$F(x) = \sum_{i=1}^{N}\sum_{j=1}^{N_{exp}} \frac{[Y_{(exp)i,j} - Y_{(cal)i,j}]^2}{NN_{exp}} \tag{2}$$

where,

N=Number of lumps

N_{exp}=Number of experimental points

$Y_{i\,(exp)}$ and $Y_{i\,(cal)}$ values of weight fraction for experimental and calculates lump i on water-free basis.

The unanimously accepted reaction path for the methanol conversion to hydrocarbons is

$$CH_3OH \underset{H_2O}{\overset{-H_2O}{\Leftrightarrow}} CH_3OCH_3 \xrightarrow{-H_2O} \text{Light oleffins} \rightarrow \begin{cases} \text{Paraffins} \\ \text{Aromatics} \end{cases}$$

Based on this, the three models used for MTG process are discussed below:

1. Model-I

The basis for this model was proposed by [24] for the disappearance of DME over ZSM-5 catalyst. The reaction model is represented as follows:

$$A \xrightarrow{k_1} B \tag{3}$$

$$A + B \xrightarrow{k_2} B \tag{4}$$

$$B \xrightarrow{k_3} C \tag{5}$$

where A represents (Oxygenates (methanol+DME)), B (Olefins) and C (aromatics+paraffins) for methanol to hydrocarbon conversion reaction. This model takes into account the autocatalytic nature of the reactions and considers the reaction rate of disappearance of methanol and DME by reaction of oxygenates with olefins [24]. The kinetic equations for the above model have been formulated by considering the elementary steps for the mechanism and are given in Eqs. (6) and (7) in terms of mass fraction (Y) of species and space time ($\tau = W/F_{A0}$):

$$\frac{-dY_A}{d\tau} = k_1 Y_A + k_2 Y_A Y_B \tag{6}$$

$$\frac{dY_B}{d\tau} = k_1 Y_A + k_2 Y_A Y_B - k_3 Y_B \tag{7}$$

The above equations were solved simultaneously using a fourth order Runge-Kutta method as discussed before. The experimental data were fitted at all the temperatures. The final kinetic constants after best fitting are given in Eqs. (8), (9) and (10), respectively.

$$k_1 = 1.093 \times 10^{13} \exp\left(-\frac{103697}{RT}\right) \tag{8}$$

$$k_2 = 8.45 \times 10^{9} \exp\left(-\frac{80606}{RT}\right) \tag{9}$$

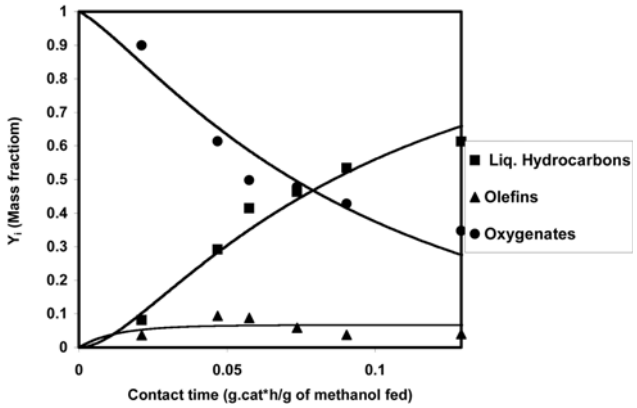

Fig. 9(a). Comparison between experimental results and simulated mass fractions (water free basis) of lumps of Model-I (T= 635 K).

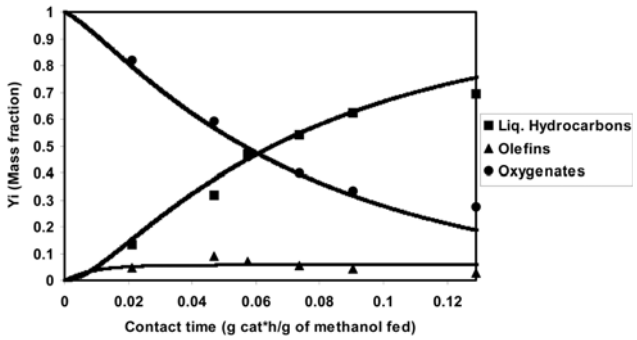

Fig. 9(b). Comparison between experimental results and simulated values of mass fraction (water free basis) of lumps of Model-I (T=653 K).

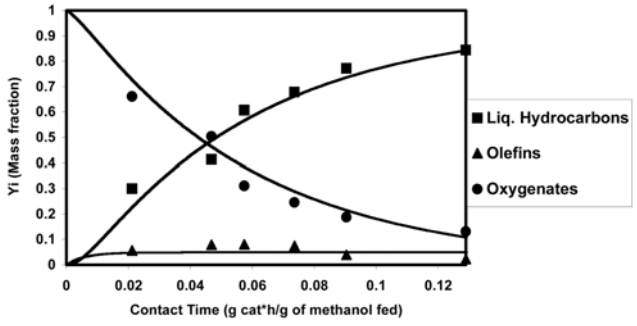

Fig. 9(c). Comparison between experimental results and simulated values of mass fraction (water free basis) of lumps Model-I (T=673 K).

$$k_3 = 3.967\times10^{6}\exp\left(-\frac{67989}{RT}\right) \tag{10}$$

A comparison between experimental data of the weight fraction (water free basis) of oxygenates, light olefins and rest of the hydrocarbons and the values calculated from the model has been plotted at different contact time. As can be seen from Figs. 9(a) to (c), the model proposed by Eqs. (6) and (7) adequately fits the experimental data. The parity plot between experimental and calculated mass fractions at different contact times and temperatures is also shown in Fig. 9(d).

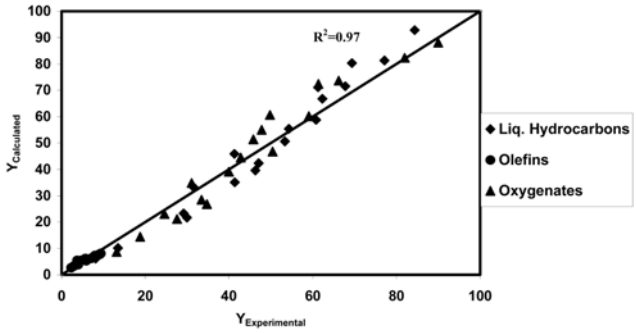

Fig. 9(d). Parity plot showing the simulated vs experimental mass fractions of hydrocarbons, olefins and oxygenates on water-free basis over HZ (Ox) catalyst using Model-1 [W/ F_{A0} (g cat*h/g methanol fed)=0.129-0.0268, T=635-673 K, P=1 atm].

The weighted least square analysis method was used to calculate the difference between experimental and simulated values. The deviation between experimental and simulated values was 1.1%. This model is simple, establishes olefins as primary products, and proposes the reaction between oxygenates and the olefins as an autocatalytic step.

2. Model-II

A third model was proposed based on the model developed by [26]. This model has also been used in MTG process by Mobil oil for simulation of a pilot plant with a fixed bed reactor.

This model also assumes that dimethyl ether and methanol are in equilibrium at all times in the reactor. Once the dimethyl ether is formed, it can react to form light olefins (major component being (C_2-C_3) which can oligomerize to form products in the gasoline boiling range. These products can react with DME/methanol or more light olefins to produce additional gasoline products. The first two reactions are assumed to be slow, while last two steps proceed rapidly. The overall reaction sequence tends to be autocatalytic. Based on these observations the kinetic scheme of MTG process may be written as:

$$2CH_3OH \underset{-H_2O}{\overset{-H_2O}{\Leftrightarrow}} CH_3OCH_3 \qquad \text{(at equilibrium)}$$

$CH_3OCH_3 \rightarrow H_2O$+Light olefins (ethylene and propylene)

Light olefins$\rightarrow$(Liquid hydrocarbons)

Light olefins+Products$\rightarrow$Liquid hydrocarbons.

The equations may be written as

$$A \xrightarrow{k_1} C \tag{22}$$

$$2C \xrightarrow{k_2} D \tag{23}$$

$$A + D \xrightarrow{k_3} D \tag{24}$$

$$C + D \xrightarrow{k_4} D \tag{25}$$

where C denotes the light olefins (ethylene and propylene), A denotes the oxygenates and D denotes that gasoline range hydrocarbons. For a fixed bed reactor the kinetic equations for these reactions have

been formulated considering elementary steps for mechanism and in terms of mass fraction.

$$\frac{-dY_A}{d\tau} = k_1 Y_A + k_3 Y_A Y_D \quad (26)$$

$$\frac{dY_C}{d\tau} = k_1 Y_A - k_2 Y_C^2 - k_4 Y_C Y_D \quad (27)$$

The Y_i represents weight fractions of component (lumped) i (on a water-free basis), τ is the space time (W/F_{A0}). The model parameters were evaluated by minimizing the deviation between the experimental and simulated conversions.

The kinetic constants of best fitting were

$$k_1 = 2.378\times10^7 \exp\left(-\frac{80678}{RT}\right) \quad (28)$$

$$k_2 = 7.70\times10^3 \exp\left(-\frac{10000}{RT}\right) \quad (29)$$

$$k_3 = 1.0\times10^3 \exp\left(-\frac{21840}{RT}\right) \quad (30)$$

$$k_4 = 9.07\times10^4 \exp\left(-\frac{96525}{RT}\right) \quad (31)$$

The experimental values of the weight fraction (water free basis) of oxygenate, light olefins and rest of the hydrocarbons (products) are compared with the calculated values from this model and have been plotted at different contact times. These results are presented in Figs. 9(a) to (c). As can be seen from Figs. 10(a) to (c) the model fitted reasonably well with the experimental data. A parity plot between experimental and calculated mass fractions at various contact times and temperatures is also given in Fig. 10(d). The deviation between experimental and simulated values was 0.6%. The weighted least square analysis was used to calculate the difference between experimental and simulated values using this model. The goodness of fitting of all the kinetic models proposed with the experimental results has been proven in a wide range of operating conditions.

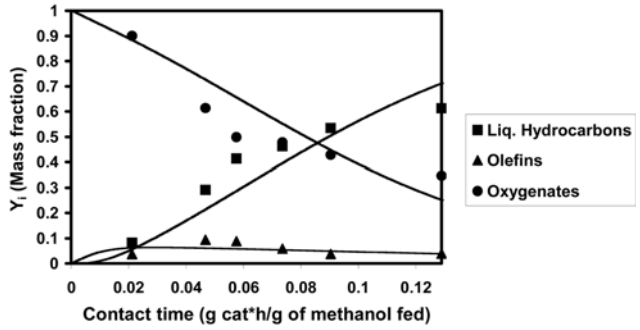

Fig. 10(a). Comparison between experimental results and simulated values of mass fraction (water-free basis) from Model-II using HZ (Ox) catalyst (T=635 K).

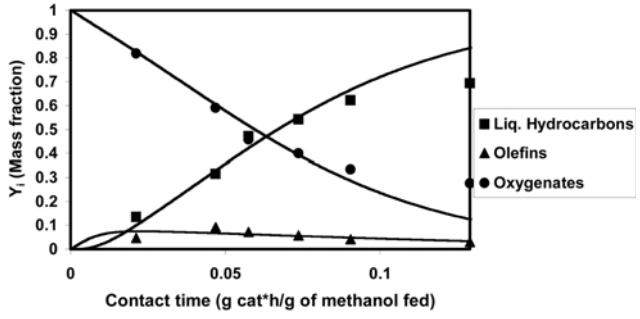

Fig. 10(b). Comparison between experimental and simulated values of mass fraction (water free basis) from Model-II with HZ (Ox) catalyst (T=653 K).

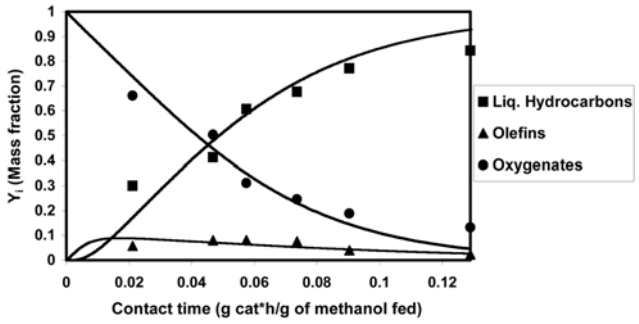

Fig. 10(c). Comparison between experimental results and simulated values of mass fraction (water-free basis) from Model-II (673 K).

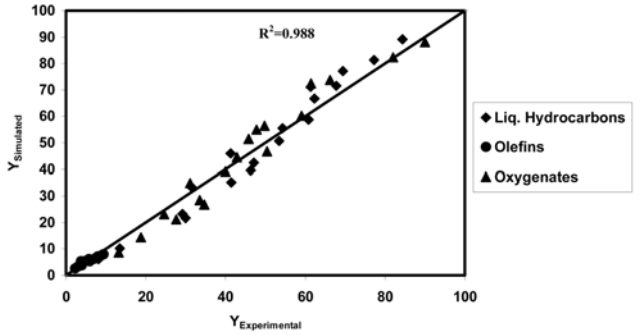

Fig. 10(d). Parity plot showing the simulated vs experimental mass fractions of hydrocarbons, olefins and oxygenates on water-free basis over HZ (Ox) using Model-II [W/F_{A0} (g cat*h/g methanol fed)=0.129-0.0268, T=635-673 K, P=1 atm].

The calculated value from the weighted least square analysis is similar for all models, the fitting being slightly better for Model (II), which was proposed from experimental results obtained under identical conditions(temperature and contact time).

CONCLUSIONS

Methanol conversion and hydrocarbons yield increased progressively on increasing W/F_{A0} with HZ (Ox). The yield of gasoline range liquid hydrocarbons increased with increase in the contact time while the yield of lighter olefins decreased. At low conversion, high yield of olefins and DME was obtained with negligible yield of aromatics. These lighter olefins and DME are partially converted to heavy hydrocarbons, indicating intermediate products in methanol to hydrocarbon reactions. Distillation profiles obtained by ASTM distillation

curves give deeper insight of composition of Indian gasoline and gasoline range hydrocarbons obtained by MTG process.

A significant effect of temperature on the methanol conversion and hydrocarbons yield was observed. There was an increase in conversion and liquid hydrocarbon yield up to 673 K, and above this major liquid product yields decreased with the increase in temperature. It was concluded that up to 673 K oligomerization, cyclization, dehydrogenation and aromatization reactions predominate and olefins are converted into the higher products. These secondary reactions convert primary olefin product to gasoline range hydrocarbons. But at temperature higher than 673 K there was cracking and rapid coke formation over the catalyst. Therefore, 673 K is the recommended temperature for MTG reaction. Yield of aromatics decreases with increase in methanol partial pressure (>90 kPa) whereas the yield of alkane and olefins marginally increases with increase in partial pressure. The validity of the kinetic models proposed has been analyzed by minimizing the error between experimental and theoretical yields of hydrocarbons.

NOMENCLATURE

A, B, C, D : abbreviated notation for lumps of various kinetic model studied
E : activation energy [kJ/mol]
F_{A0} : mass flow of methanol fed [gh^{-1}]
F(x) : objective function
k_1, k_2, k_3, k_4 : kinetic constants of individuals steps of various kinetic models [h^{-1}]
N : number of lumps
N_{exp} : number of experimental points
R : gas constant (8.314) [$Jmol^{-1}K^{-1}$]
T : temperature [K]
W : mass of catalyst [g]
Y_i : weight fraction of lump i on water free basis

Greek Letters

ρ : density [kg/m^3]
τ : contact time [g cat *h/g of methanol fed]

REFERENCES

1. E. C. Alyea and R. N. Bhat, *Zeolites*, **15**, 318 (1995).
2. V. R. Choudhary and A. K. Kinage, *Zeolites*, **15**, 732 (1995).
3. G. Calleja, A. de. Lucas and R. Van. Grieken, *Fuel*, **74**, 4451 (1995).
4. C. D. Chang, *J. Catal.*, **86**, 289 (1984).
5. A. M. Al-Jarallah, U. A. El-Nafaty and M. M. Abdillahi, *Appl. Catal. A: Gen.*, **154**, 117 (1997).
6. D. M. M. Song, H. Fu, J. O. Ehresmann and J. F. Haw, *J. Am. Chem. Soc.*, **124**, 3844 (2002).
7. F. C. Patcas, *J. Catal*., **231**, 194 (2005).
8. J. L. Ramos, A. M. D. Farias, L. E. P. Borges, J. L. Monteiro, M. A. Fraga, S. L. Aguiar and G. Appel, *Catal. Today*, **101**, 39 (2005).
9. C. D. Chang, *Chem. Eng. Sci.*, **35**, 619 (1980).
10. J. F. Haw, W. Song, D. M. Marcus and J. B. Nicholas, *Acc. Chem.*, **36**, 317 (2003).
11. G. J. Hutchings, G. W. Watson and D. J. Willock, *Micro. Meso. Mater.*, **29**, 67 (1999).
12. W. Kaeding and S. A. Butter, *J. Catal.*, **61**, 155 (1980).
13. M. M. Abdillahi, U. A. El-Nafaty and A. M. Al-Jarallah, *Appl. Catal. A: Gen.*, **91**, 1 (1992).
14. O. Dewaele, V. L. Geers, G. F. Froment and G. B. Marin, *Chem. Eng. Sci.*, **54**, 4385 (1999).
15. A. J. Marchi and G. F. Froment, *Appl. Catal. A: Gen.*, **94**, 91 (1993).
16. K. Nishi, T. Shimizu, H. Yoshida, A. Satsuma and Hattori, *Appl. Catal. A: Gen.*, **166**, 335 (1998).
17. F. J. Keil, *Micro. Meso. Mater.*, **29**, 49 (1999).
18. D. Freeman, R. P. K. Wells and G. J. Hutchings, *J. Catal.*, **205**, 358 (2002).
19. Y. Inoue, K. Nakashiro and Y. Ono, *Micro. Meso. Mater.*, **4**, 379 (1995).
20. Ø. Mikkelsen and S. Kolboe, *Micro. Meso. Mater.*, **29**, 173 (2002).
21. H. Schoenfleder, J. Hinder, J. Werther and F. J. Keil, *Chem. Eng. Sci.*, **49**, 5377 (1994).
22. M. Stöcker, *Micro. Meso. Mater.*, **38**, 279 (2000).
23. U. Sedran, A. Mahay and H. I. D. Lasa, *Chem. Eng. Sci.*, **45**, 1161 (1990).
24. M. Chen and W. J. Reagan, *J. Catal.*, **59**, 123 (1979).
25. A. G. Gayubo, P. L. Benito, A. T. Aguayo, I. Aguirre and J. Bilbao, *Chem. Eng. J.*, **63**, 45 (1996).
26. P. H. Schipper and F. J. Kramback, *Chem. Eng. Sci.*, **41**, 1013 (1986).
27. A. G. Gayubo, A. T. Aguayo, A. E. Sánchez del Campo, A. M. Tarrio and J. Bilbao, *Ind. Eng. Chem. Res.*, **39**, 292 (2000).
28. R. S. Mihail, G. Satraja, Maria, G. Musca and G. Pop, *Chem. Eng. Sci.*, **38**, 1581 (1983).
29. H. A. Zaidi and K. K. Pant, *Catal. Today*, **96**, 155 (2004).
30. H. A. Zaidi and K. K. Pant, *Korean J. Chem. Eng.*, **22**, 353 (2005).
31. H. A. Zaidi and K. K. Pant, *Ind. Eng. Chem. Res.*, **47**, 2970 (2008).
32. A. T. Aguayo, A. G. Gayubo, M. Castilla, J. Marandes, M. Olazar and J. Bilbao, *Ind. Eng. Chem. Res.*, **40**, 6087 (2001).